Search for Photoproduction of Axion-like Particles at GlueX

Yunjie Yang
Massachusetts Institute of Technology
on behalf of the GlueX collaboration

1st Workshop on New Light Physics and Photon-beam Experiments
March 8—10, 2021

Outline

- Motivation and introduction
- Analysis overview
  - Dataset and event selection
  - Mass resolution function
  - Acceptance and efficiency
  - Signal search
- Summary

Motivation: ALPs

- Axion-like particles (ALPs) are hypothetical pseudoscalars found in many proposed extensions to the Standard Model (SM):
  - strong CP problem
  - hierarchy problem
  - a portal connecting SM and dark matter

$$\mathcal{L} \supset -\frac{4\pi\alpha_s c_g}{\Lambda} a G^{\mu\nu}\tilde{G}_{\mu\nu}$$

- ALP couplings to the SM gauge bosons are highly suppressed at low energies by a large cut-off scale Λ.

- Recent model building efforts have led to considerable interest for ALPs with masses in the ***MeV-to-GeV scale***, relevant for accelerator-based experiments
  - e.g. Hook *et al.* introduces a strongly-coupled mirror sector => solving *the strong CP problem* while evading the *axion quality problem* at the same time

A. Hook, S. Kumar, Z. Liu, R. Sundrum. PRL 124 221801 (2020). arXiv: 1911.12364

Motivation: GeV-scale ALPs

- The phenomenology of ALP-gluon coupling for GeV-scale ALP is dominated by hadronic interactions and needed to be understood.
- A novel data-driven approach was proposed to determine the hadronic interaction strengths for GeV-scale ALPs [1] (*cf.* D. Aloni's talk in this workshop)
- The phenomenology of the photoproduction of GeV-scale ALPs was explored in the context of PrimEx (for ALP-photon coupling) and GlueX (for ALP-gluon coupling) [2] (*cf.* D. Aloni's talk in this workshop)
- This model was selected by the Physics Beyond Collider study at CERN as one of its primary benchmark models [1901.09966].

[1] D. Aloni, Y. Soreq, M. Williams. PRL 123, 031803 (2019). arXiv: 1811.03474
[2] D. Aloni, C. Fanelli, Y. Soreq, M. Williams. PRL 123, 071801 (2019). arXiv: 1903.03586

Phenomenology of GeV-scale ALPs

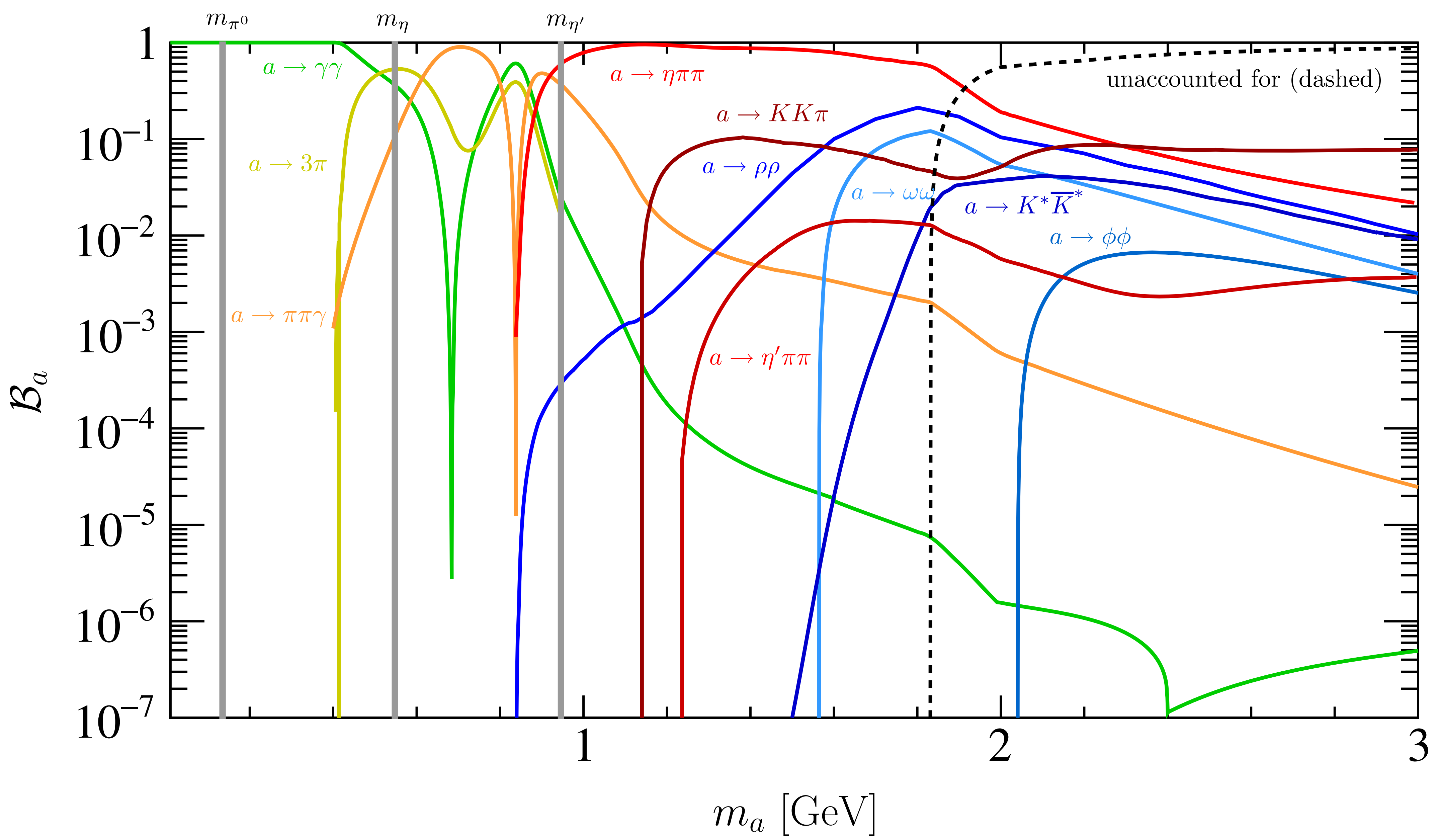

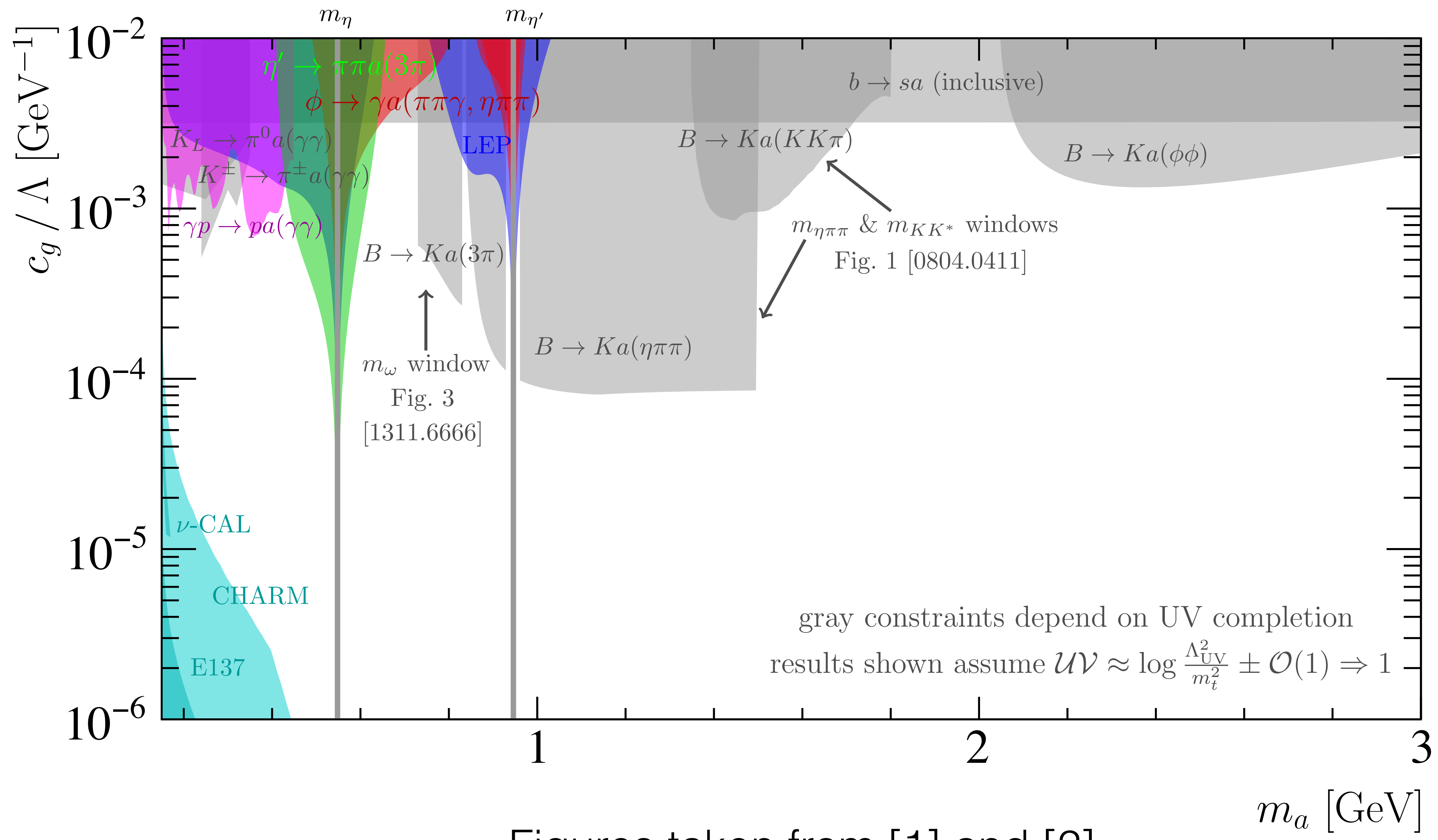

Figures taken from [1] and [2]

- ALPs mix with the SM pseudoscalars (e.g., π^0, η, η') and decay in similar modes
- GlueX can set world-leading limits in ALP-gluon coupling strengths in certain regions of ALP masses $\lesssim$ 1GeV
- The magenta limit is set in [2] using results from the first GlueX published paper [3]

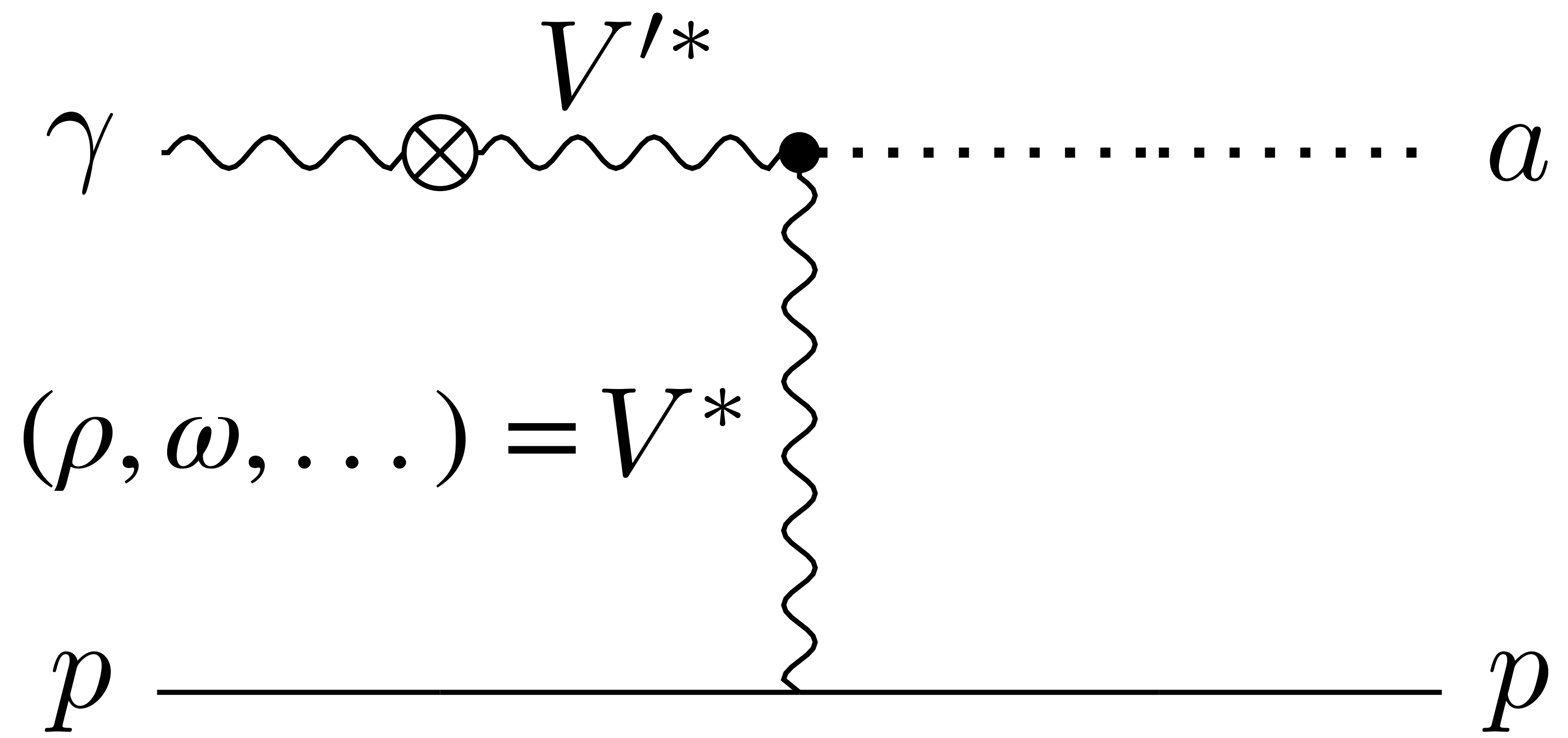

[1] D. Aloni, Y. Soreq, M. Williams. PRL 123, 031803 (2019). arXiv: 1811.03474
[2] D. Aloni, C. Fanelli, Y. Soreq, M. Williams. PRL 123, 071801 (2019). arXiv: 1903.03586
[3] GlueX collaboration. Phys. Rev. C 95, 042201 (2017). arXiv: 1701.08123

GlueX experiment

- Located in Hall D of Jefferson Lab
- Photon beam:
  - produced by coherent bremsstrahlung of CEBAF electron beam off of a thin diamond radiator
  - tagged high intensity beam: $5 \times 10^7\,\gamma/s$
- A fixed target experiment:
  - Liquid hydrogen target
  - $\sqrt{s} \approx 4$ GeV
- GlueX spectrometer:
  - 2T solenoid magnet
  - hermetic angular coverage
  - tracking, calorimetry, particle identification: $e^{\pm}, \pi^{\pm}, K^{\pm}, p^{\pm}, \gamma$

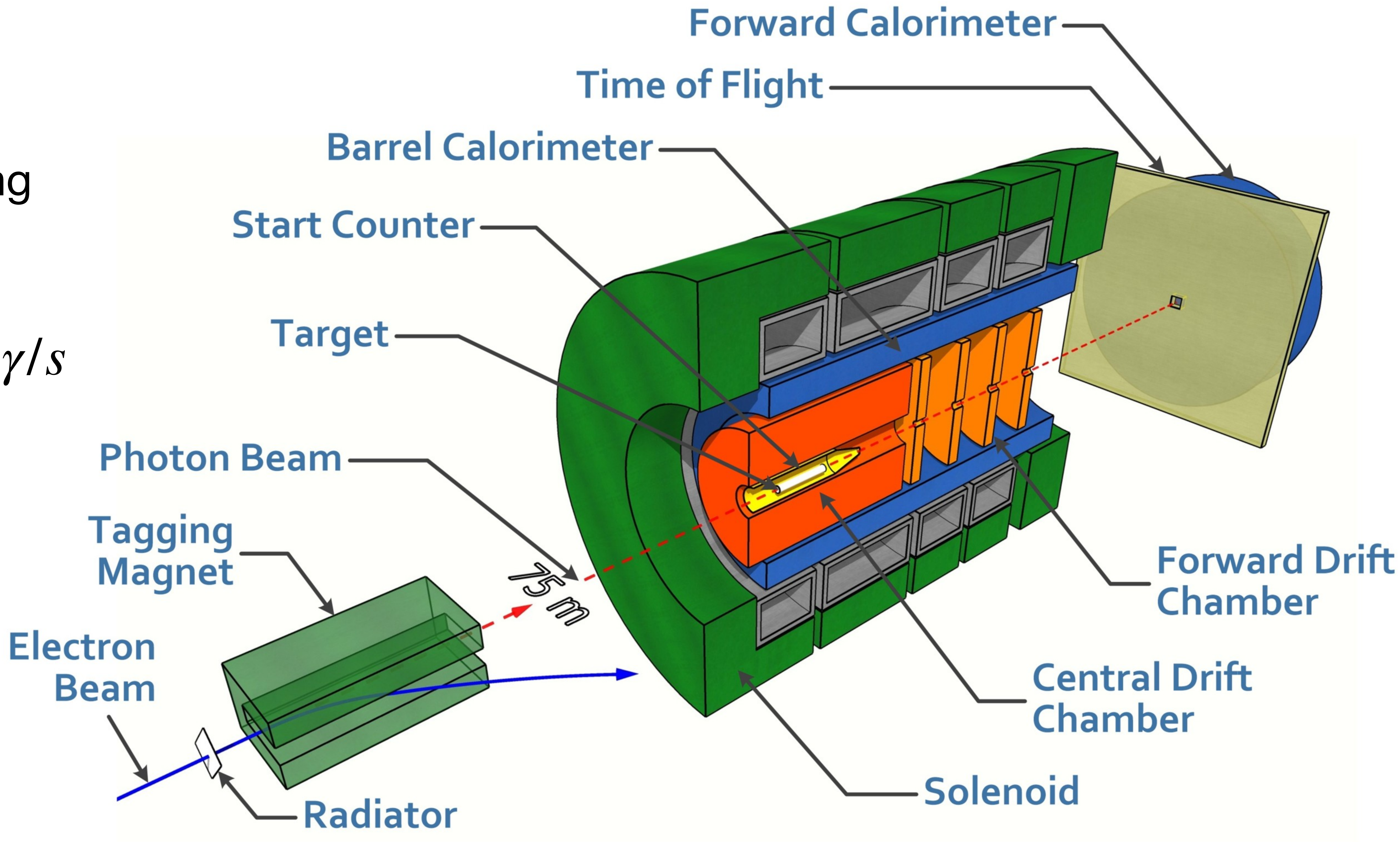

Figure taken from [4]

[4] GlueX collaboration. NIMA 987, 164807 (2021). arXiv: 2005.14272

Analysis overview

- We will analyze two reaction channels of $\gamma p \to pX$:
  - $X = \gamma\gamma$ to search for ALPs between π^0 and η
  - $X = \pi^+\pi^-\pi^0$ to search for ALPs between η and ω
- Bump hunts will be performed over the $\gamma\gamma$ and $\pi^+\pi^-\pi^0$ mass spectra to obtain, at each mass, upper limits on the ALP yield (the searches are currently blinded).
- The upper limits on the ALP yield can then be used to place upper limits on the ALP-gluon coupling constant c_g/Λ at each ALP mass.
- The expected ALP yield in a bin of [s, t] is worked out in [2] (using $\gamma\gamma$ channel as an example):

$$n_a(s,t) \approx \left(\frac{f_\pi}{f_a}\right)^2 \left[|\langle \boldsymbol{a\pi^0} \rangle|^2 \frac{n_{\pi^0}(s,t)\epsilon(m_a,s,t)}{\mathcal{B}(\pi^0 \to \gamma\gamma)\epsilon(m_\pi,s,t)} + |\langle \boldsymbol{a\eta} \rangle|^2 \frac{n_\eta(s,t)\epsilon(m_a,s,t)}{\mathcal{B}(\eta \to \gamma\gamma)\epsilon(m_\eta,s,t)} \right] \mathcal{B}(a \to \gamma\gamma)$$

[2] D. Aloni, C. Fanelli, Y. Soreq, M. Williams. PRL 123, 071801 (2019). arXiv: 1903.03586

Analysis overview: theory inputs

pion and ALP **decay constants**

$$n_a(s,t) \approx \boxed{\left(\frac{f_\pi}{f_a}\right)}^2 \left[|\langle \boldsymbol{a\pi^0} \rangle|^2 \frac{n_{\pi^0}(s,t)\epsilon(m_a,s,t)}{\mathcal{B}(\pi^0 \to \gamma\gamma)\epsilon(m_\pi,s,t)} + |\langle \boldsymbol{a\eta} \rangle|^2 \frac{n_\eta(s,t)\epsilon(m_a,s,t)}{\mathcal{B}(\eta \to \gamma\gamma)\epsilon(m_\eta,s,t)} \right] \mathcal{B}(a \to \gamma\gamma)$$

The ALP decay constant is related to the ALP-gluon coupling constant c_g and the cut-off scale Λ by:

$$f_a = -\frac{\Lambda}{32\pi^2 c_g}$$

Analysis overview: theory inputs

$$n_a(s,t) \approx \left(\frac{f_\pi}{f_a}\right)^2 \left[\boxed{|\langle \boldsymbol{a\pi^0} \rangle|}^2 \frac{n_{\pi^0}(s,t)\epsilon(m_a,s,t)}{\mathcal{B}(\pi^0 \to \gamma\gamma)\epsilon(m_\pi,s,t)} + \boxed{|\langle \boldsymbol{a\eta} \rangle|}^2 \frac{n_\eta(s,t)\epsilon(m_a,s,t)}{\mathcal{B}(\eta \to \gamma\gamma)\epsilon(m_\eta,s,t)} \right] \mathcal{B}(a \to \gamma\gamma)$$

mass-dependent **ALP-pseudoscalar mixing terms** worked out in [1]

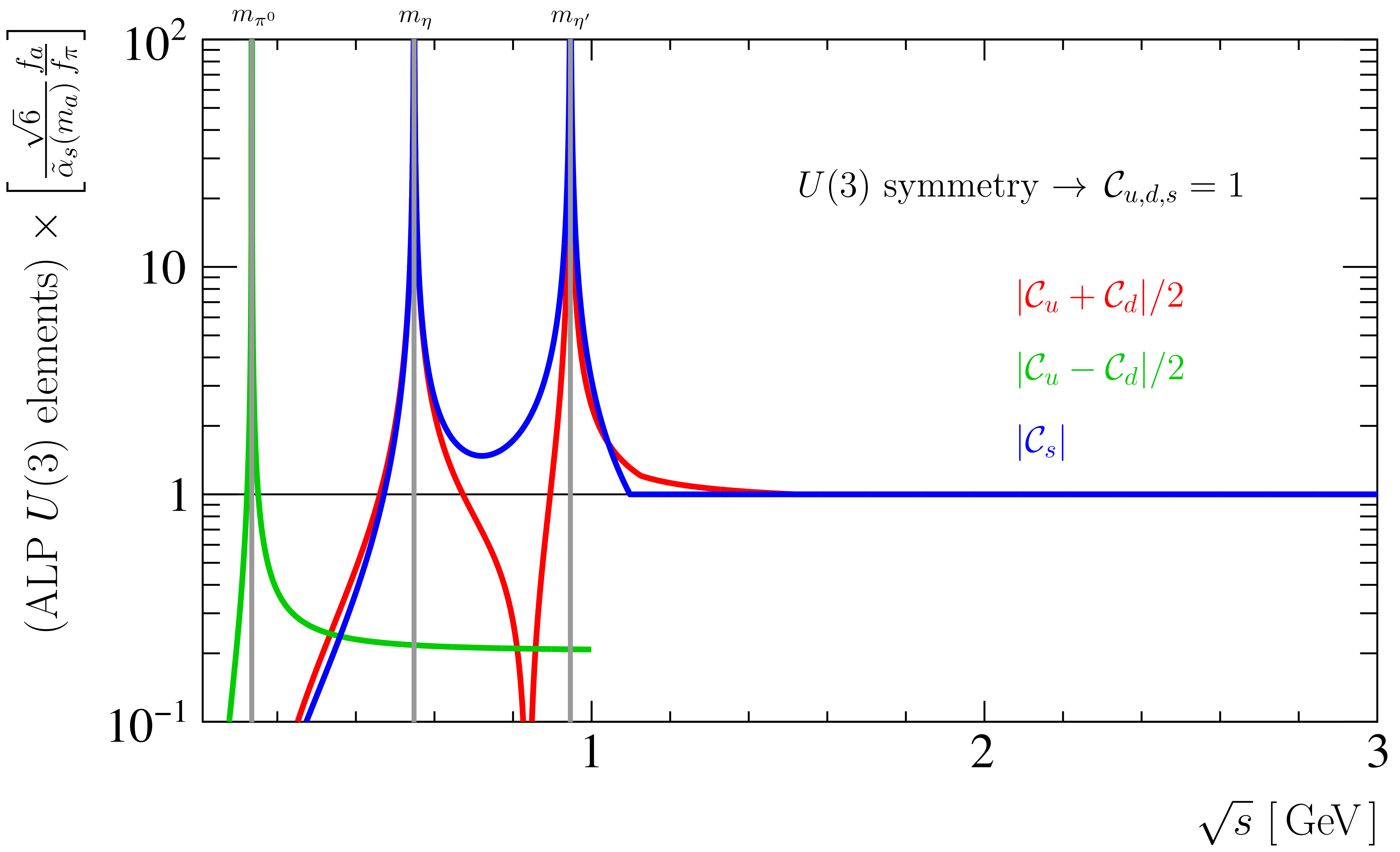

[1] D. Aloni, Y. Soreq, M. Williams. PRL 123, 031803 (2019). arXiv: 1811.03474

Analysis overview: theory inputs

$$n_a(s,t) \approx \left(\frac{f_\pi}{f_a}\right)^2 \left[|\langle \boldsymbol{a\pi^0} \rangle|^2 \frac{n_{\pi^0}(s,t)\epsilon(m_a,s,t)}{\boxed{\mathcal{B}(\pi^0 \to \gamma\gamma)}\epsilon(m_\pi,s,t)} + |\langle \boldsymbol{a\eta} \rangle|^2 \frac{n_\eta(s,t)\epsilon(m_a,s,t)}{\boxed{\mathcal{B}(\eta \to \gamma\gamma)}\epsilon(m_\eta,s,t)} \right] \boxed{\mathcal{B}(a \to \gamma\gamma)}$$

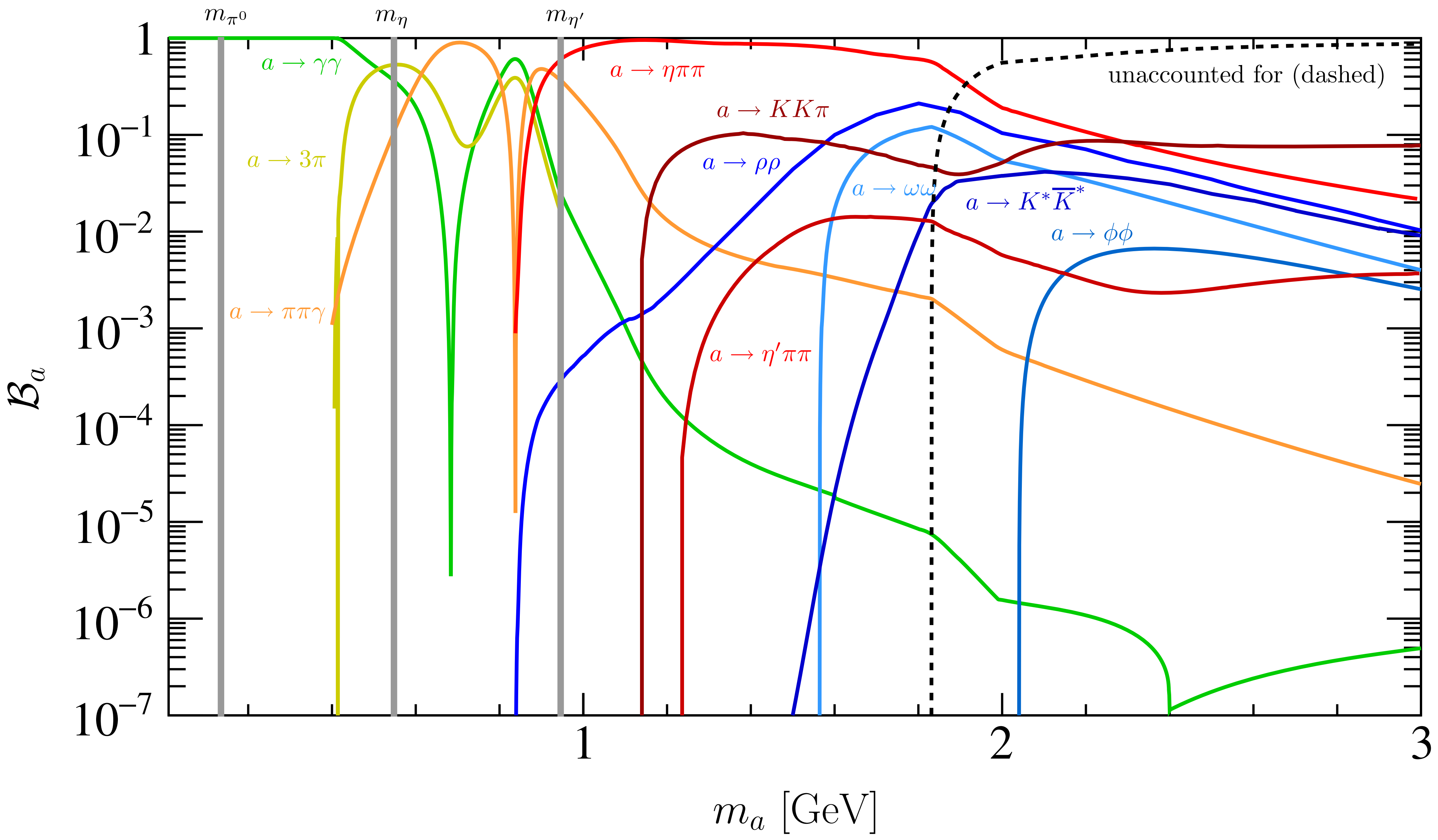

branching fractions from PDG or worked out in [1]

[1] D. Aloni, Y. Soreq, M. Williams. PRL 123, 031803 (2019). arXiv: 1811.03474

Analysis overview: experimental inputs

π^0 **and** η **yields** in an $[s, t]$ bin

$$n_a(s,t) \approx \left(\frac{f_\pi}{f_a}\right)^2 \left[|\langle \boldsymbol{a\pi^0} \rangle|^2 \frac{n_{\pi^0}(s,t)\,\epsilon(m_a,s,t)}{\mathcal{B}(\pi^0 \to \gamma\gamma)\,\epsilon(m_\pi,s,t)} + |\langle \boldsymbol{a\eta} \rangle|^2 \frac{n_\eta(s,t)\,\epsilon(m_a,s,t)}{\mathcal{B}(\eta \to \gamma\gamma)\,\epsilon(m_\eta,s,t)} \right] \mathcal{B}(a \to \gamma\gamma)$$

mass-dependent **acceptance × efficiency** ratios of ALP to π^0 and η

Additionally, **mass resolution function** is needed in the signal component of the model PDF in the signal search

Dataset and event selection

- Dataset: full GlueX Phase-I dataset used, $\sim 170\, pb^{-1}$ (in selected E_γ range)
- Event selection follows a sensitivity-based strategy without examining the evidence for an ALP signal in order to avoid experimenter bias.
- Selection includes:
  - E_γ: [8, 9] GeV and |-t|: [0.15, 1] GeV^2
  - Exclusivity cuts of the reaction:
    - kinematic fit quality
    - missing mass squared of the reaction
    - no extra tracks and extra energy < 100 MeV in the event
  - Reconstruction quality cuts on individual objects or the reaction

Mass spectra and normalization fits

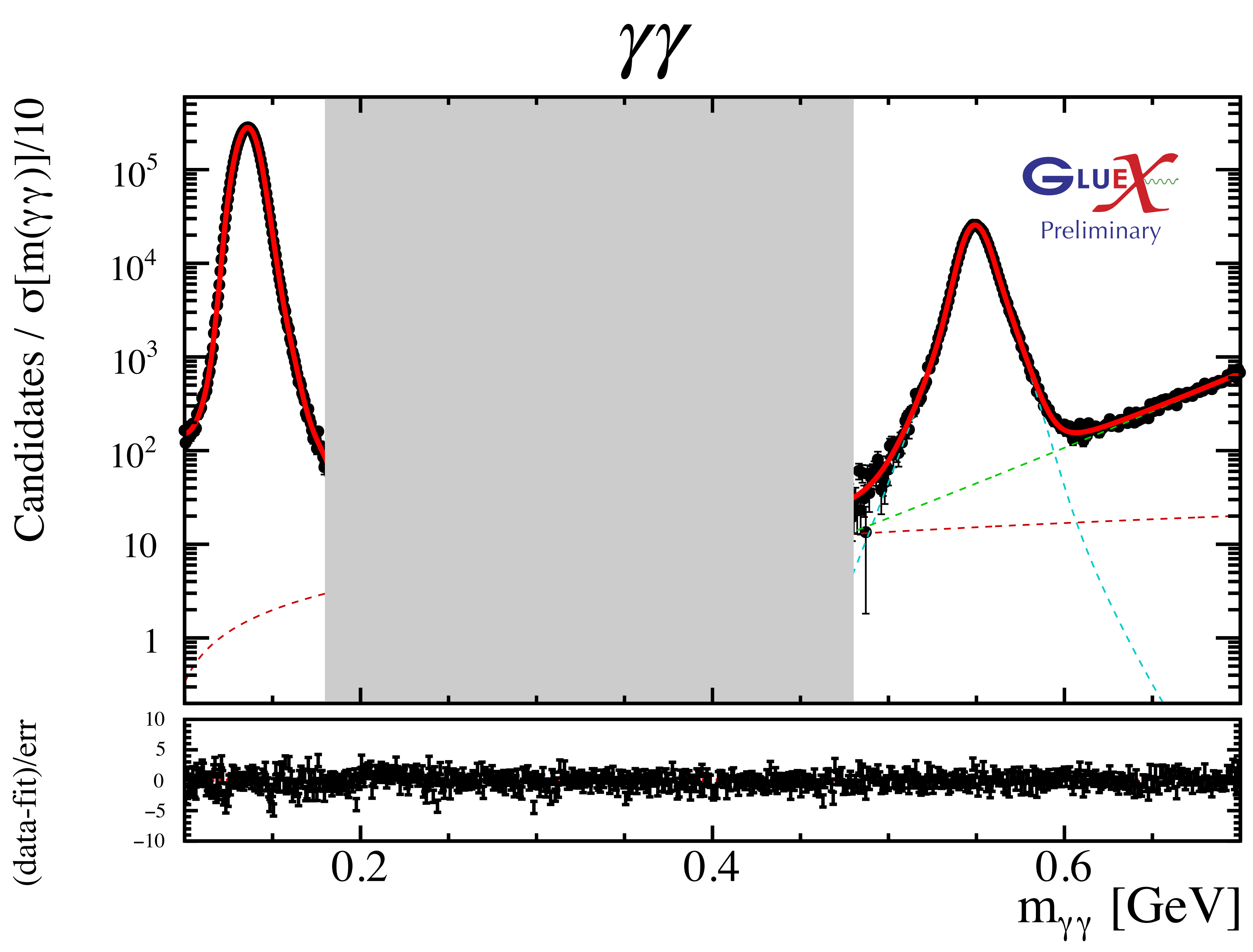

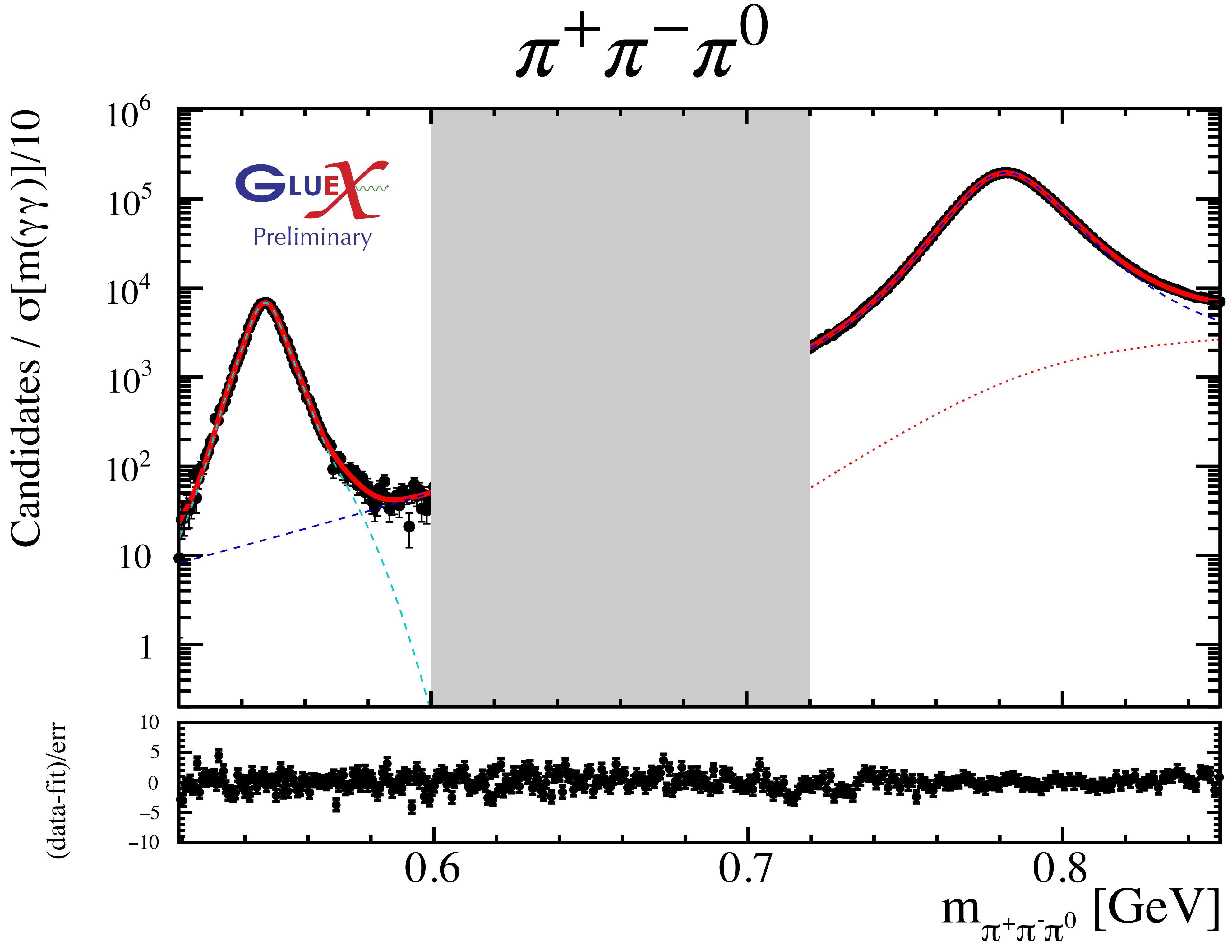

- Fit model components:
  - Resonances: sums of Crystal Ball functions and Gaussians
  - Background: ($\gamma\gamma$) linear component + ω tail or ($\pi^+\pi^-\pi^0$) power-law function of the energy released (Q)
  - Additional floating signal component (for blinding stage only), but no information reported
- Residuals account for both accidental subtraction and a modeling uncertainty for the large resonance PDFs

Mass resolution function

- MCs are used to obtain both the **mass resolution function** and the mass-dependent **acceptance × efficiency** ratios.
- MC datasets of ALPs with different masses m_a are generated over the search regions.
- Mass resolution functions extracted from MC samples:
  - a data-driven correction is applied to match MC resolutions to those observed in data for π^0, η, and ω mesons

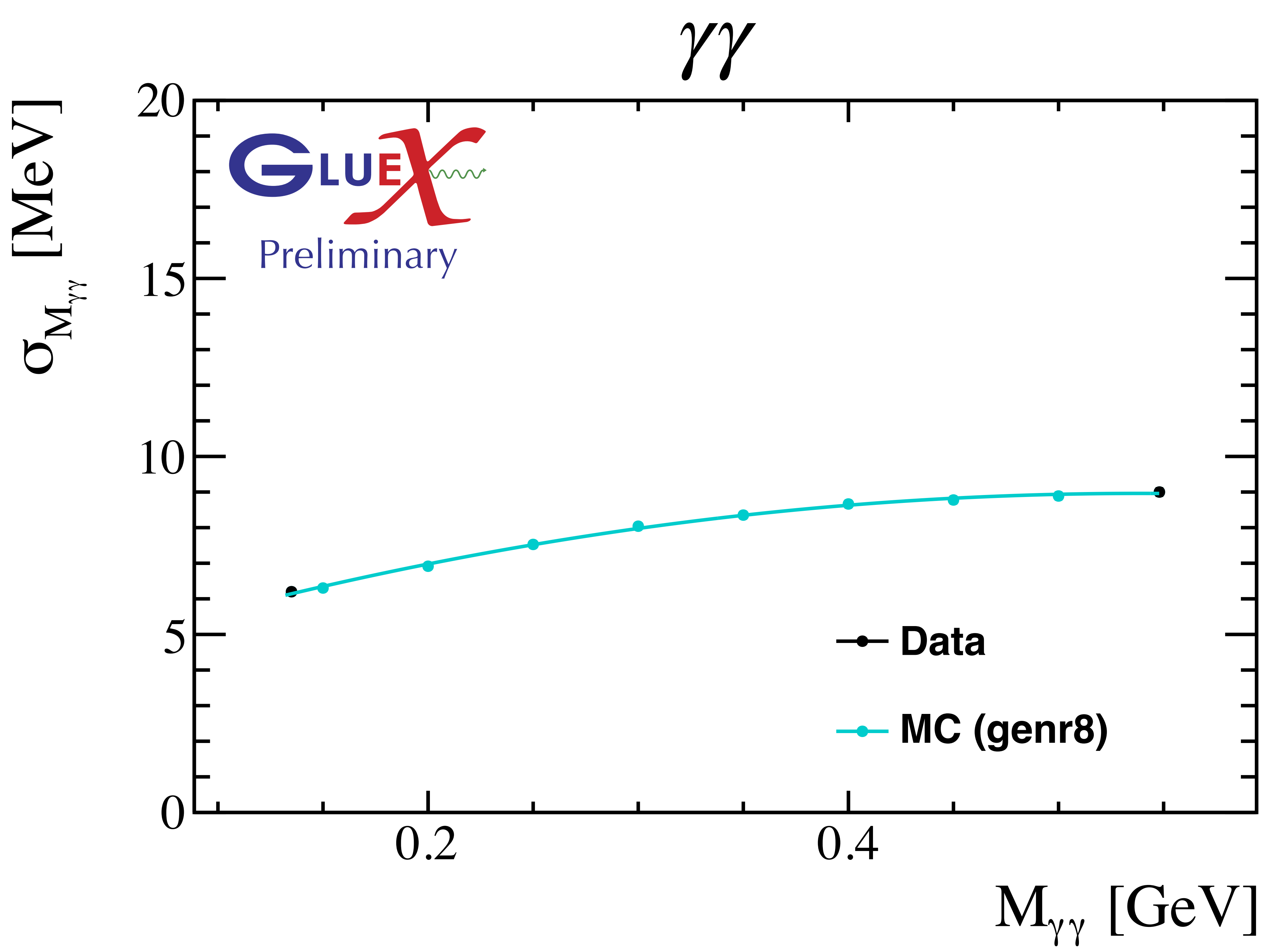

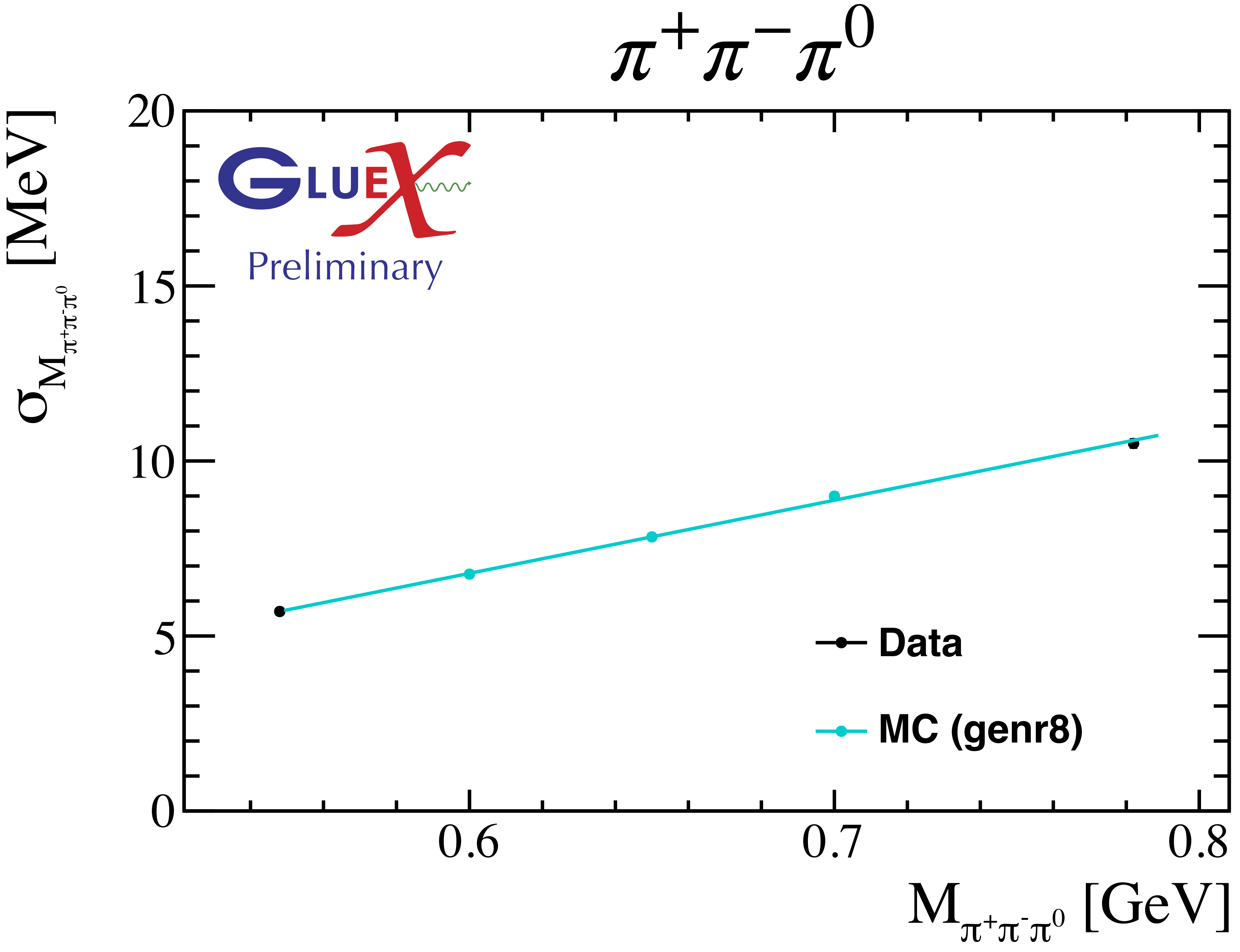

Acceptance × efficiency

- Only ***ratios*** of acceptance × efficiency enter the ALP normalization equation.
- Acceptance:
  - the probability that a reaction producing an ALP in a [s, t] bin will have all final-state particles in the fiducial region;
  - strong dependence on both m_a and t; a phase space Monte Carlo procedure is employed to quantify this effect
- Efficiency:
  - the probability for the particles to be reconstructed if they are in the fiducial region
  - minimal dependence on m_a and t; the choice of fiducial region is designed to minimize such dependence

$$n_a(s,t) \approx \left(\frac{f_\pi}{f_a}\right)^2 \left[|\langle \boldsymbol{a\pi^0} \rangle|^2 \frac{n_{\pi^0}(s,t)\epsilon(m_a,s,t)}{\mathcal{B}(\pi^0 \to \gamma\gamma)\epsilon(m_\pi,s,t)} + |\langle \boldsymbol{a\eta} \rangle|^2 \frac{n_\eta(s,t)\epsilon(m_a,s,t)}{\mathcal{B}(\eta \to \gamma\gamma)\epsilon(m_\eta,s,t)} \right] \mathcal{B}(a \to \gamma\gamma)$$

Acceptance × efficiency

- Only ***ratios*** of acceptance × efficiency enter the ALP normalization equation.
- Maps of acceptance × efficiency are constructed by interpolating between the generated ALP MCs and used in the ALP normalization.

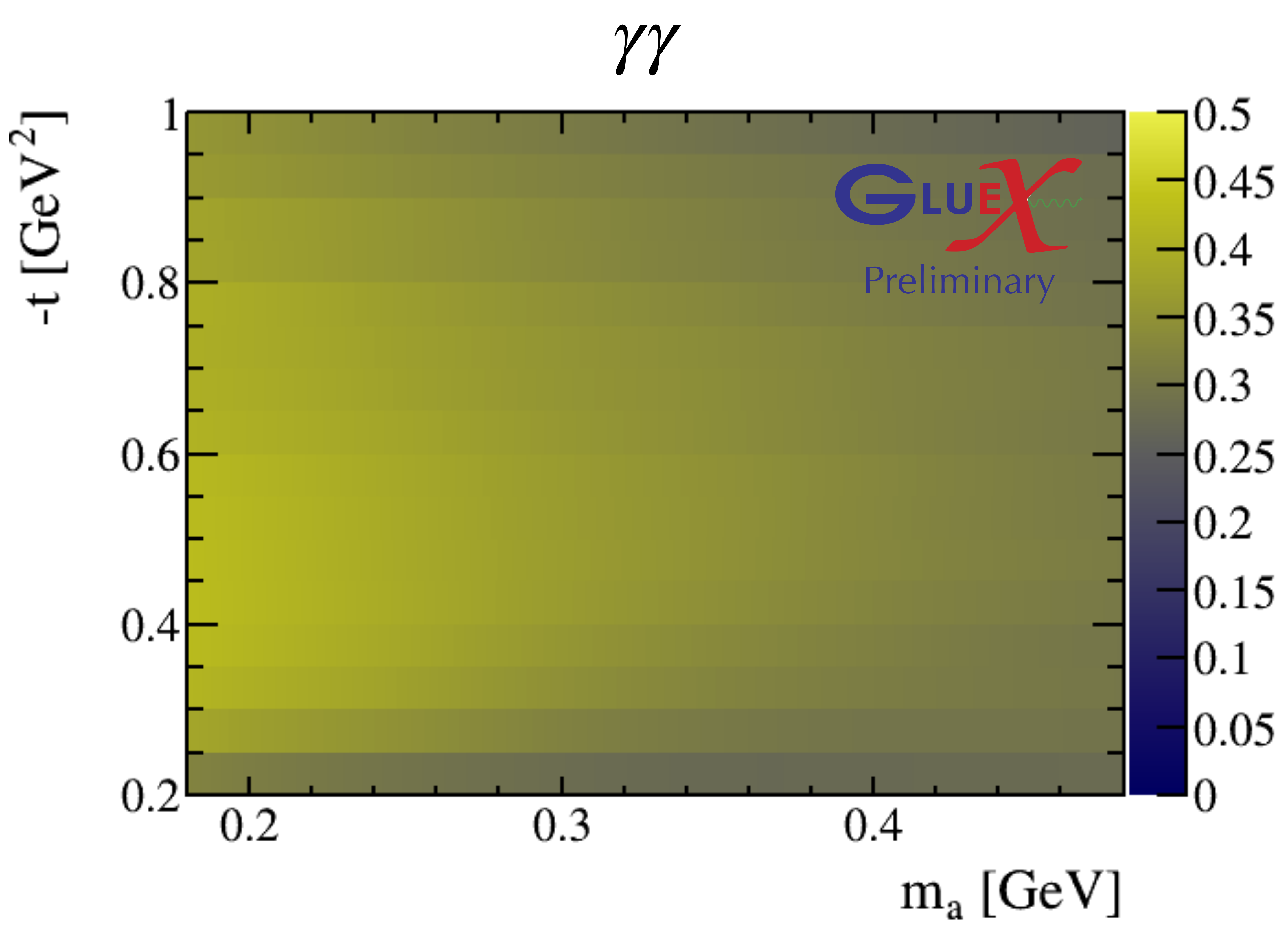

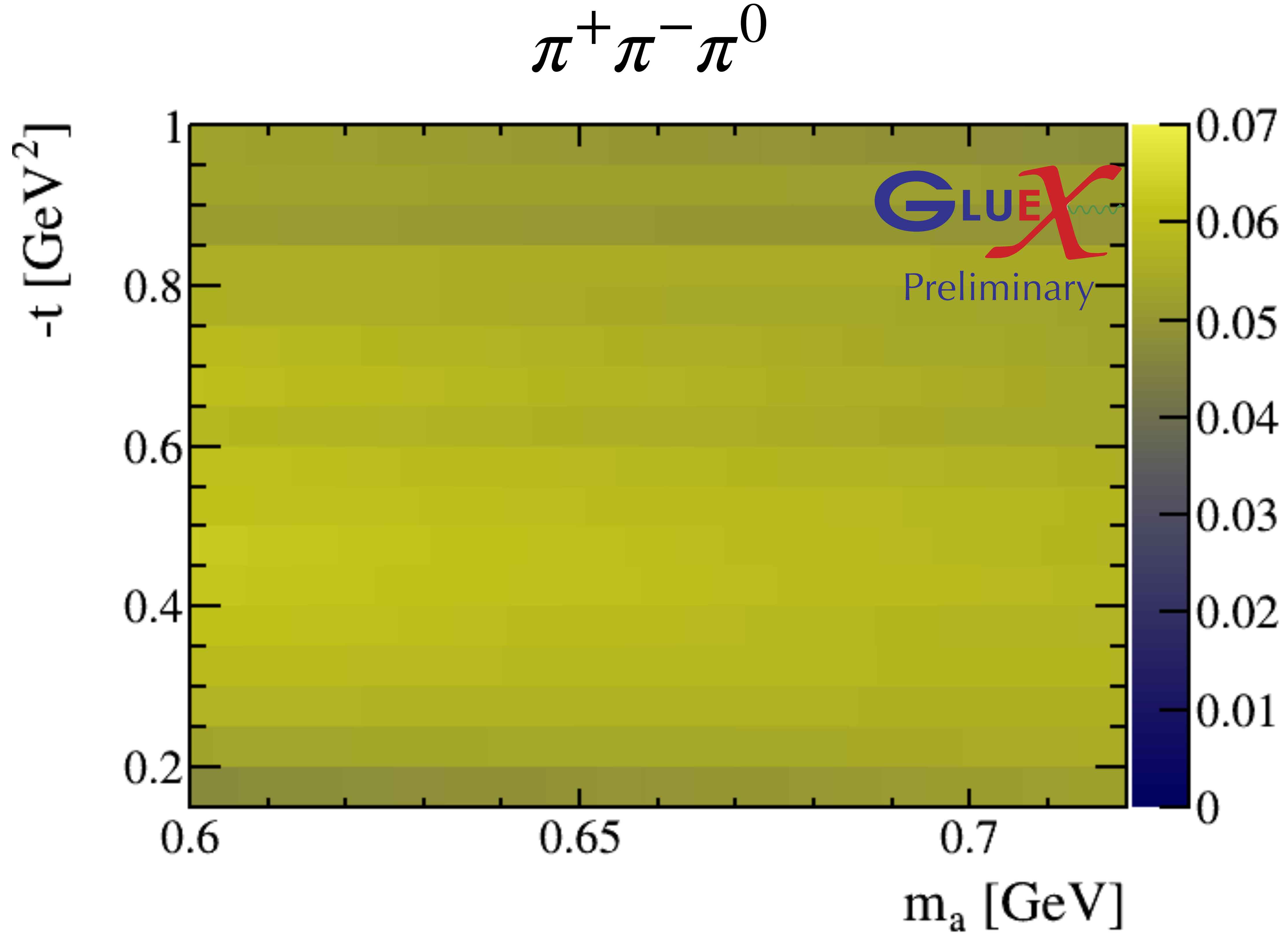

Signal search

- The signal search, i.e., bump hunt, will follow the strategy outlined by Williams [5] and done in LHCb dark photon searches [6, 7] and general dimuon resonance searches [8] and others [9, 10].
- The strategy **rewards goodness of fit** while **punishing model complexity** by adding a penalty term to the likelihood; confidence interval (CI) of the signal estimator is obtained from a **profile** of the penalized likelihood
- The search is currently blinded (hence the cut-off at +2 on the figures) and the procedure is validated using an ensemble generated from the background-only fit model to the data.

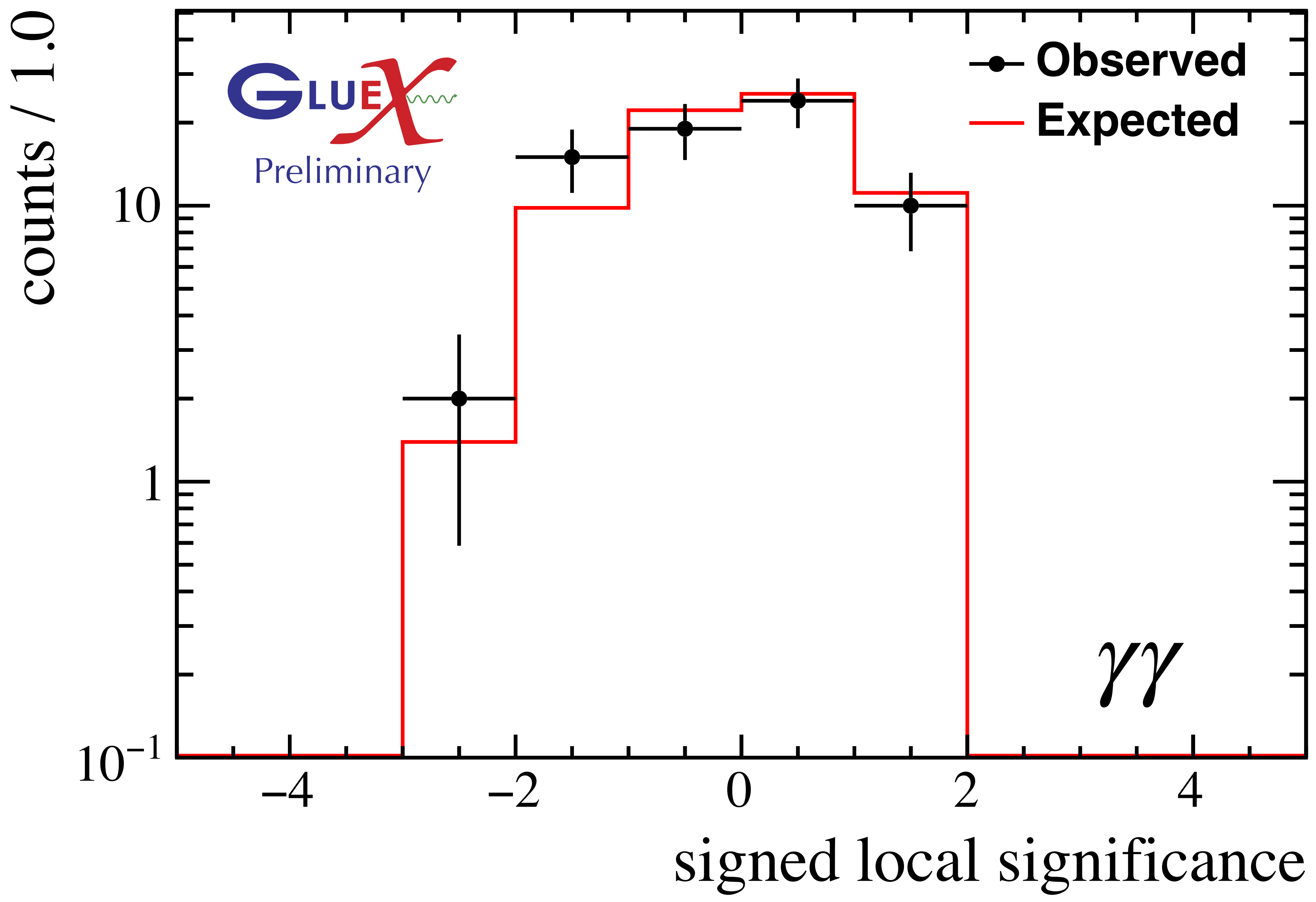

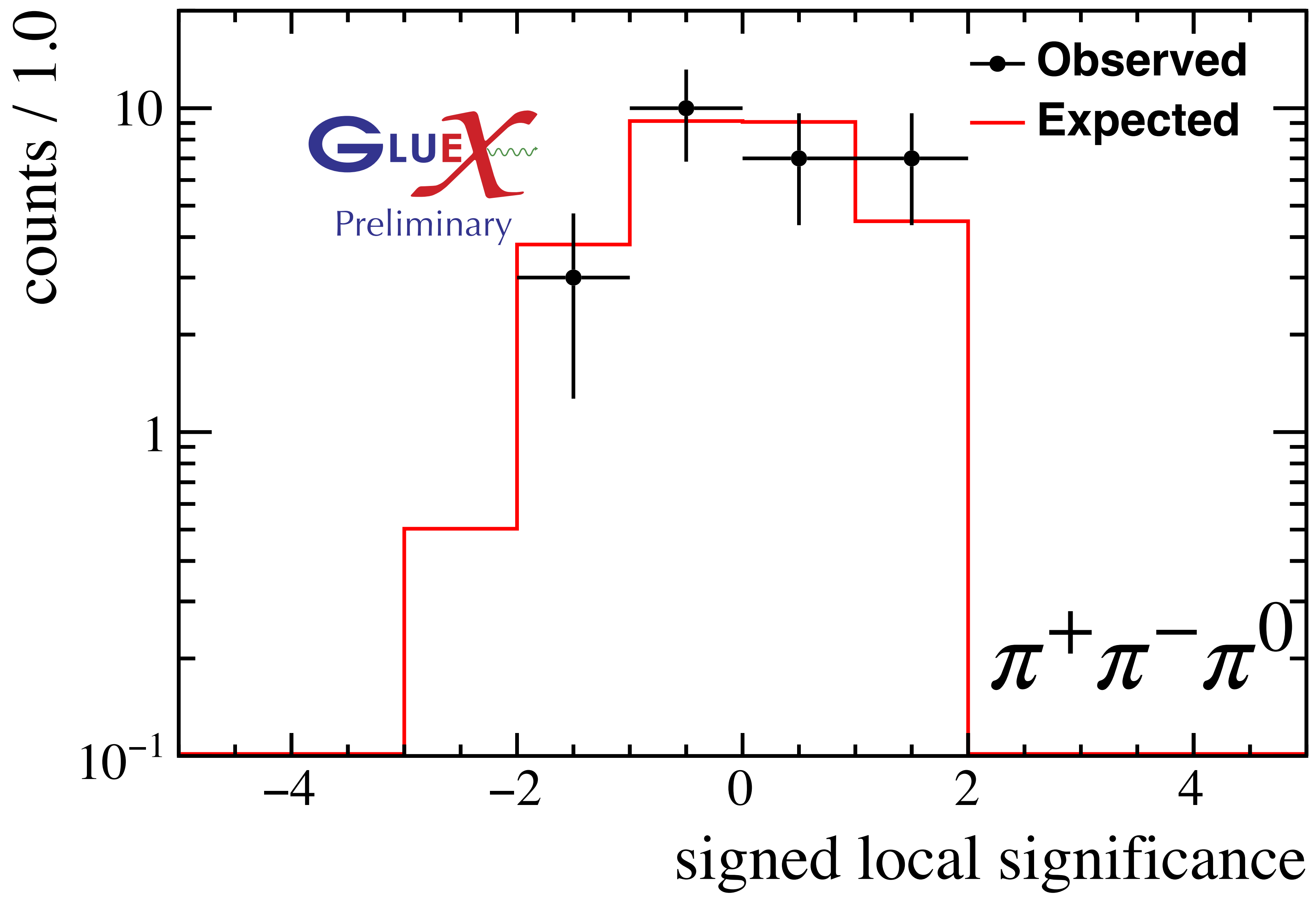

[5] M. Williams. JINST 12, P09034 (2017). arXiv: 1705.03578
[6] LHCb collaboration. PRL 120, 061801 (2018). arXiv: 1710.02867
[7] LHCb collaboration. PRL 124, 041801 (2020). arXiv: 1910.06926
[8] LHCb collaboration. JHEP 10 (2020)156. arXiv: 2007.03923
[9] C. Cesarotti, Y. Soreq, M. J. Strassler, J. Thaler, W. Xue. PRD 100, 015021 (2019). arXiv:1902.04222
[10] J. Landay, M. Mai, M. Döring, H. Haberzettl, K. Nakayama. PRD 99, 016001 (2019). arXiv:1810.00075

Systematic uncertainties

- ALP yield:
  - Signal model: mass resolution function and shape of the unknown signal
  - Background model: incorporated in the signal search procedure with model index as nuisance parameter
- Normalization:
  - Acceptance × efficiency: dominated by acceptance
  - π^0 and η yields: evaluated with different signal and background shapes
  - Branching fractions: PDG

$$n_a(s,t) \approx \left(\frac{f_\pi}{f_a}\right)^2 \left[|\langle \boldsymbol{a\pi^0} \rangle|^2 \frac{n_{\pi^0}(s,t)\epsilon(m_a,s,t)}{\mathcal{B}(\pi^0 \to \gamma\gamma)\epsilon(m_\pi,s,t)} + |\langle \boldsymbol{a\eta} \rangle|^2 \frac{n_\eta(s,t)\epsilon(m_a,s,t)}{\mathcal{B}(\eta \to \gamma\gamma)\epsilon(m_\eta,s,t)} \right] \mathcal{B}(a \to \gamma\gamma)$$

Source	$a \to \gamma\gamma$	$a \to \pi^+\pi^-\pi^0$
Signal model	1%	1%
Background model	2–10%	2–8%
Acceptance×efficiency	3–6%	5%
π^0 and η yields	3%	1%
Branching fractions	0.1–0.5%	1.5%
Total	5–12%	5–9%

Preliminary

Those specified as a range are m_a-dependent.

Results: expected sensitivity

- GlueX is expected to set ***world-leading limits*** in ALP-gluon coupling strengths in regions of the ALP phase space, using only $170\,pb^{-1}$ of data.

- Note: the gray constraints are taken from [1] which assume $\mathcal{O}$(TeV) UV scale and have $\mathcal{O}(1)$ uncertainties due to unknown UV physics.

- This search will also have sensitivity to other models, e.g. the B boson.

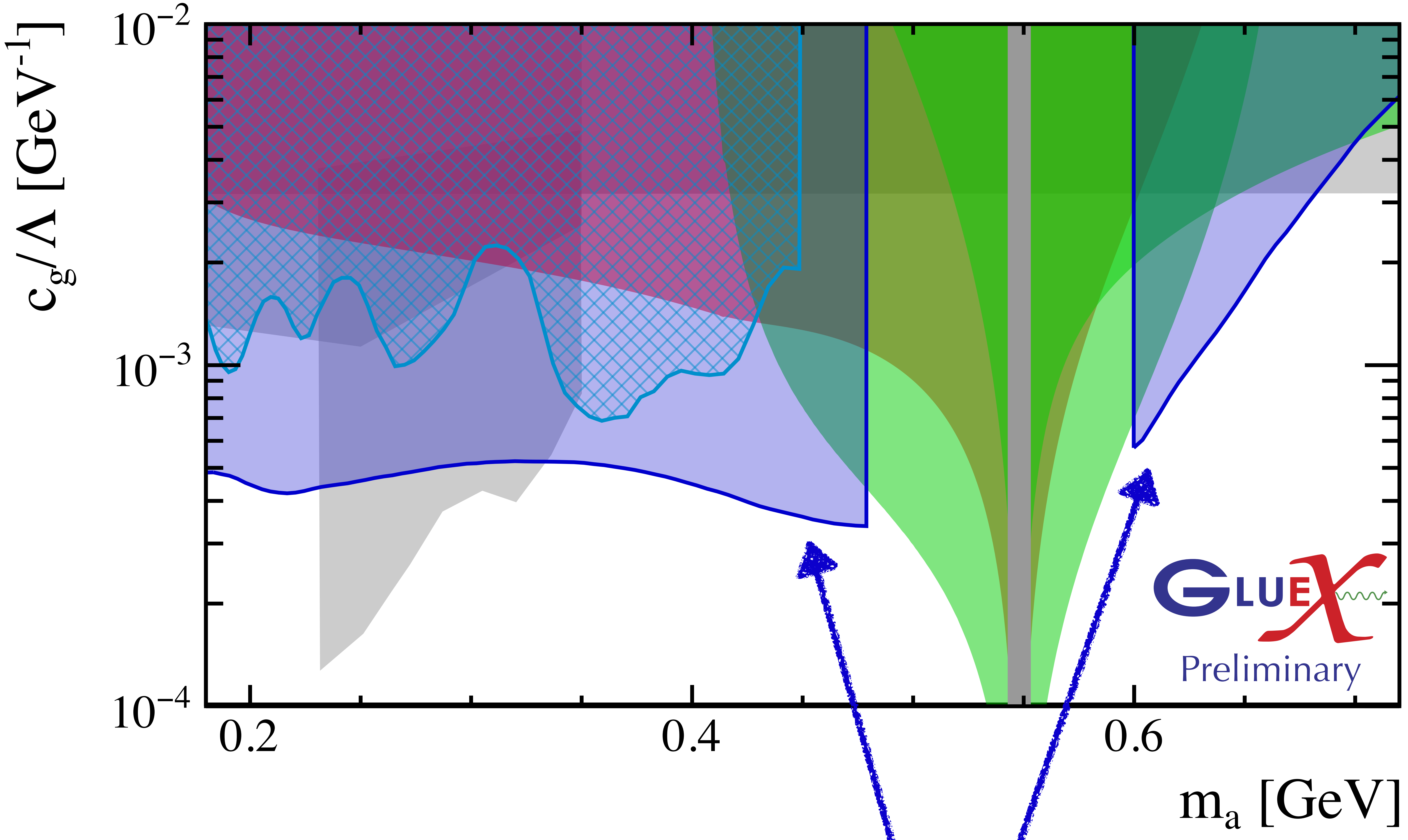

expected sensitivity from this search

Summary

- ALPs are hypothetical pseudoscalars found in many proposed extensions to the Standard Model; MeV-to-GeV scale ALPs have received considerable interest recently.
- We are conducting a search for ALPs in $\gamma\gamma$ and $\pi^+\pi^-\pi^0$ channels using the GlueX Phase I dataset.
- The search is expected to set world-leading limits in regions of the phase space on the ALP-gluon coupling.
- The analysis is under collaboration review. Stay tuned!

Backup

Sensitivity projection

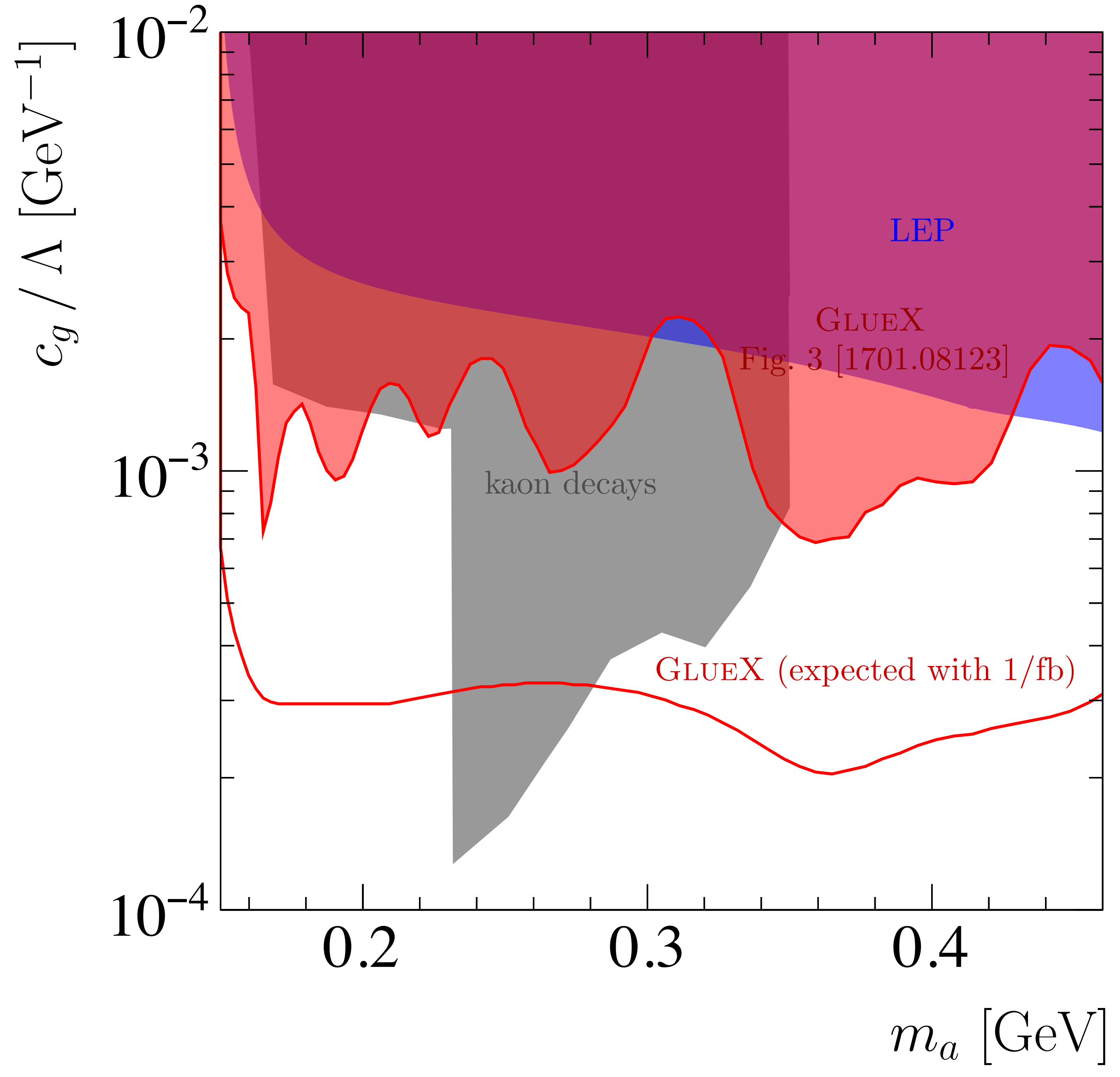

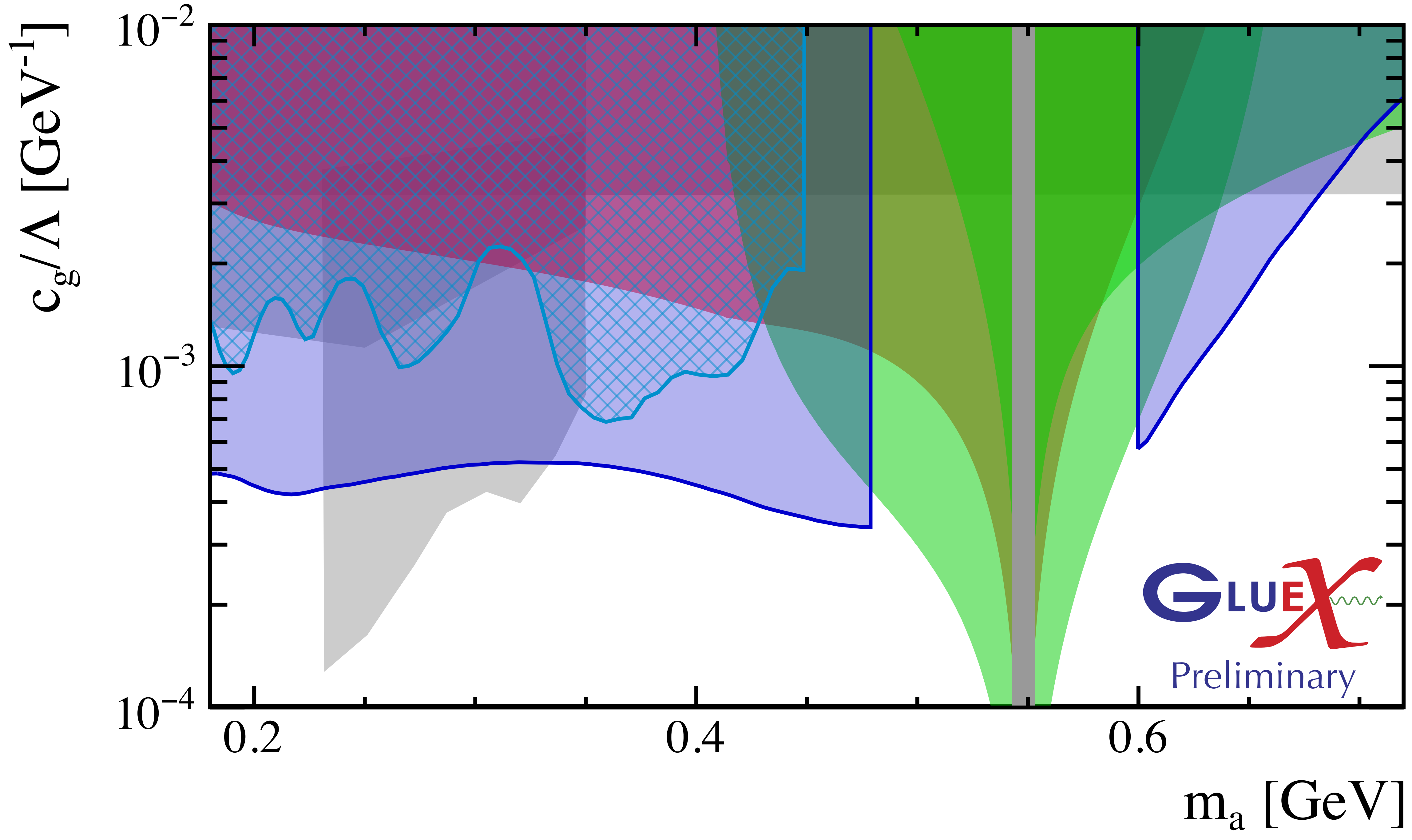

- Sensitivity scales as $\mathscr{L}^{1/4}$
- The expected sensitivity from this search, using 0.17/fb of data, is consistent with (and probably a little bit better) than the prediction shown in the left figure, taken from [2], for 1/fb of GlueX data.

[2] D. Aloni, C. Fanelli, Y. Soreq, M. Williams. PRL 123, 071801 (2019). arXiv: 1903.03586

ALP mixing

The low-mass ALP U(3) representation is given by [1811.03474]:

$$\boldsymbol{a} = \langle \boldsymbol{a\pi^0} \rangle \boldsymbol{\pi}^0 + \langle \boldsymbol{a\eta} \rangle \boldsymbol{\eta} + \langle \boldsymbol{a\eta'} \rangle \boldsymbol{\eta'},$$

$$\langle \boldsymbol{a\pi^0} \rangle \approx \frac{\delta_I}{2} \frac{m_a^2}{m_a^2 - m_\pi^2},$$

$$\langle \boldsymbol{a\eta} \rangle \approx \left[\frac{m_a^2}{\sqrt{6}} - \frac{m_{\pi^0}^2}{2\sqrt{6}} \right] \frac{1}{m_a^2 - m_\eta^2},$$

$$\langle \boldsymbol{a\eta'} \rangle \approx \left[\frac{m_a^2}{2\sqrt{3}} - \frac{m_{\pi^0}^2}{\sqrt{3}} \right] \frac{1}{m_a^2 - m_{\eta'}^2},$$

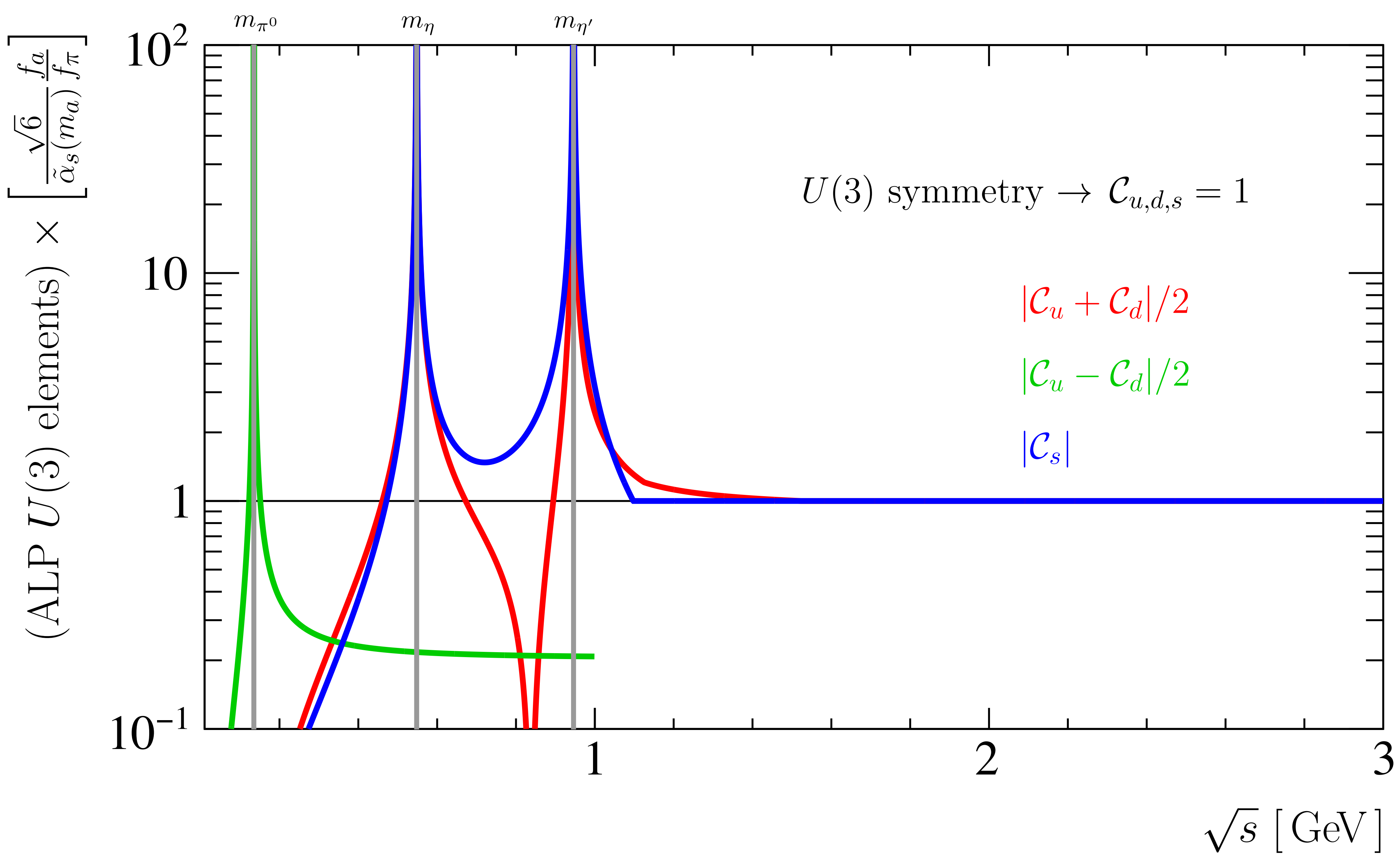

Event selection

- Event selection follows a sensitivity-based strategy:
  - Starting from the analysis trees with some loose selection as the “baseline”
  - For each selection variable under consideration, compute the expected sensitivity for a set of possible cut values
  - Choose the cut value for each variable based on the expected sensitivity and selection efficiency on π^0 and η

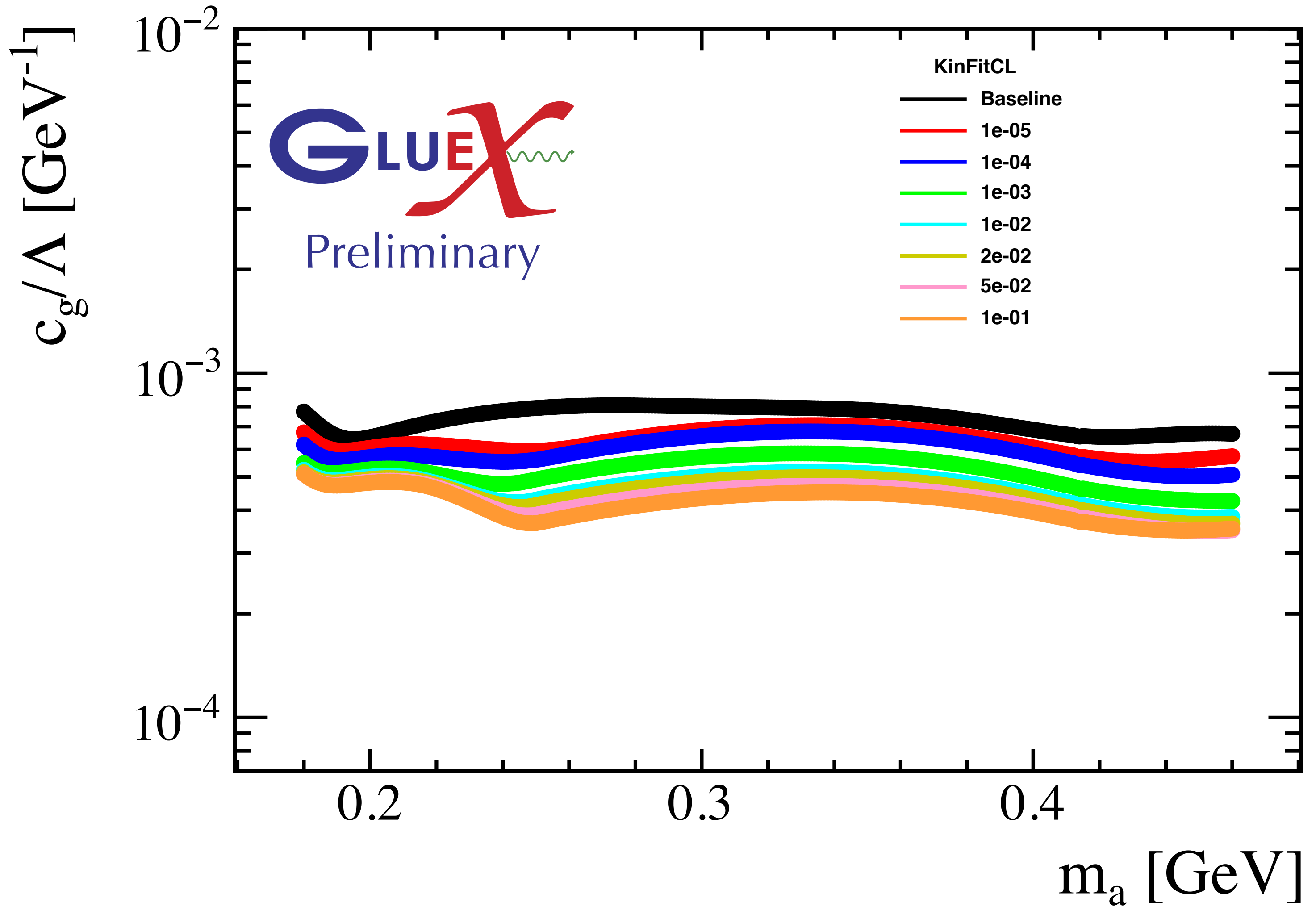

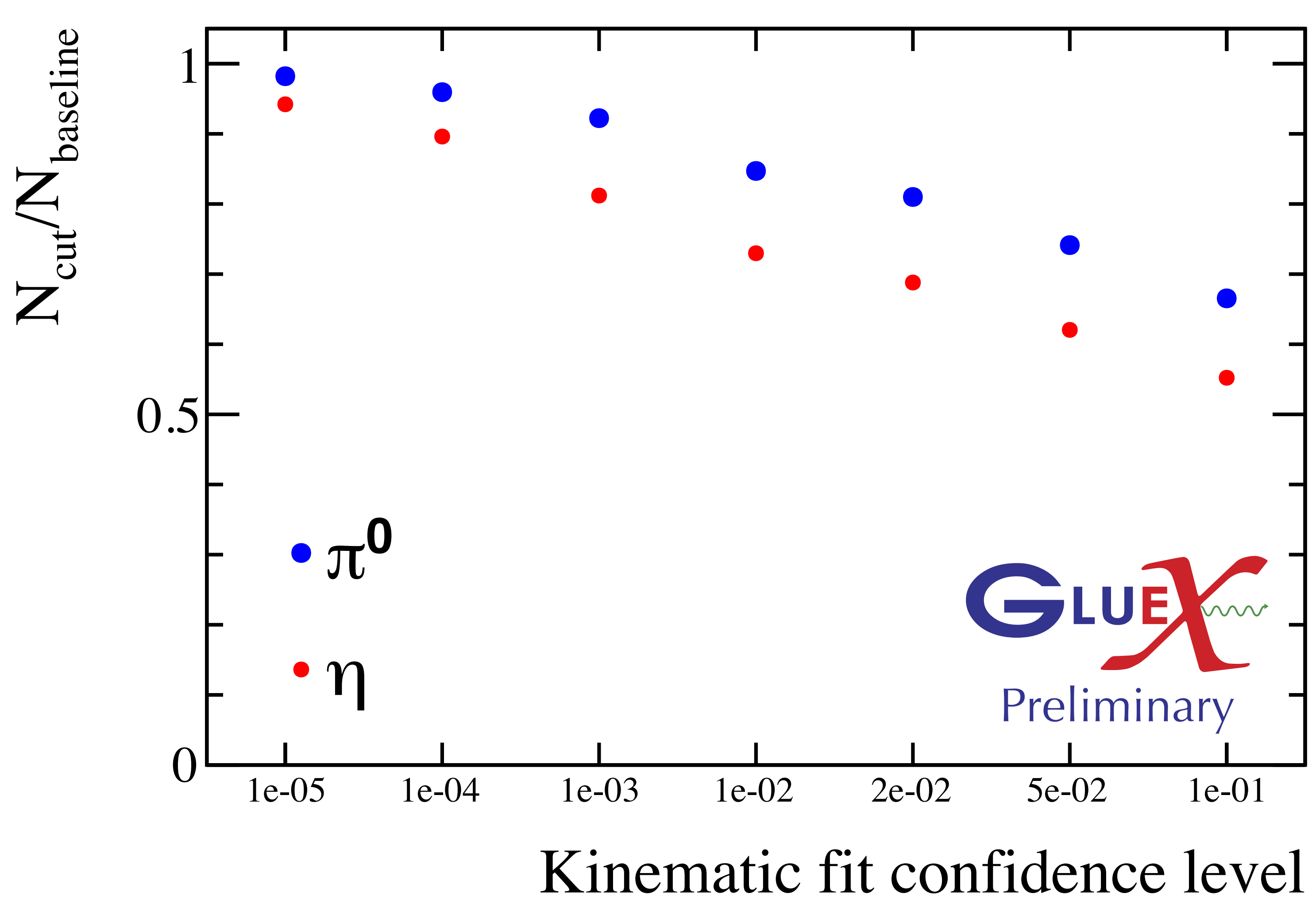

Example above: kinematic fit confidence level cut for $\gamma\gamma$ channel and 2×10^{-2} is chosen

Event selection

$\gamma\gamma$ channel

Variable Name	Baseline Selection	Optimized Selection
Beam energy	(8, 9) GeV	–
Mandelstam $-t$	(0.1, 1) GeV^2	–
Missing mass squared	(-0.05, 0.05) GeV^2	–
vertex z position	(50, 80) cm	–
vertex radial position	< 1 cm	–
proton momentum	> 0.35 GeV	–
FCAL shower radial position	(25, 100) cm	–
BCAL shower z position	(150, 380) cm	–
Number of unused tracks	0	–
Unused energy	< 0.1 GeV	–
dist$(x_4(\gamma_1), x_4(\gamma_2))$	> 0 cm	> 12 cm
photon energy	(0.1, 10) GeV	(0.5, 10) GeV
Kinematic fit confidence level	$> 10^{-7}$	> 0.02

$\pi^+\pi^-\pi^0$ channel

Variable Name	Baseline Selection	Optimized Selection
Beam energy	(8, 9) GeV	–
Mandelstam $-t$	(0.1, 1) GeV^2	–
Missing mass squared	(-0.05, 0.05) GeV^2	–
vertex z position	(50, 80) cm	–
vertex radial position	< 1 cm	–
proton momentum	> 0.35 GeV	–
FCAL shower radial position	(25, 100) cm	–
BCAL shower z position	(150, 380) cm	–
Number of unused tracks	0	–
Unused energy	< 0.1 GeV	–
photon energy	(0.1, 10) GeV	–
dist$(x_4(\gamma_1), x_4(\gamma_2))$	> 0 cm	> 12 cm
$m(\pi^0)$ (measured quantities)	(100, 170) MeV	(110, 155) MeV
Kinematic fit confidence level	$> 10^{-7}$	$> 10^{-3}$

- The fiducial region defined by the selection is designed to minimize the dependence of reconstruction efficiency on mass and t.
- All selection cuts are fairly standard and are not expected to “sculpture" peaks.

Monte Carlo simulation

- MCs are used to obtain both the **mass resolution function** and the mass-dependent **acceptance × efficiency** ratios.

- Monte Carlo samples:
  - t-channel event generator (`genr8`) + effects from other beam photons (random triggers);
  - followed by collaboration common tools for Geant4-based detector simulation (`hdgeant4`), detector response simulation (`mcsmear`) and reconstruction
  - followed by the same analysis workflow

- MC datasets of ALPs with different masses m_a are generated over the search regions.

Acceptance × efficiency

acc.*eff. from full MC | acc. from phase-space MC | recon. eff.

$\gamma\gamma$

$\pi^+\pi^-\pi^0$

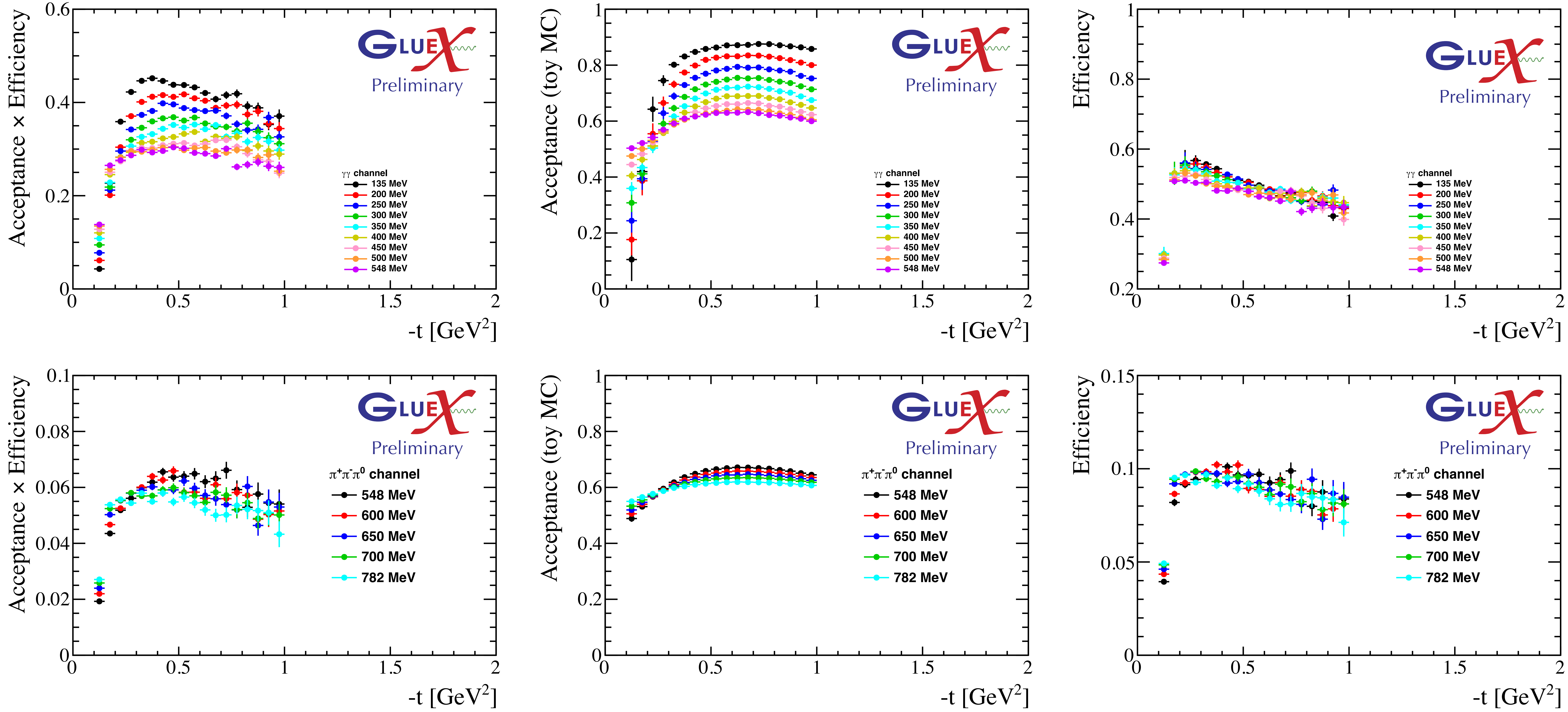

Signal search

- The signal search, i.e., bump hunt, will follow the strategy outlined by Williams [5] and done in LHCb dark photon searches [6, 7] and general dimuon resonance searches [8] and others [9, 10].
- The strategy rewards goodness of fit while punishing model complexity by adding a penalty term to the likelihood.
- Confidence Interval (CI) of the signal estimator is obtained from a profile of the penalized likelihood, where the model index m is treated as a discrete nuisance parameter.
- The total background model contains a nominal background model (to account for gross features such as the π^0 and η peaks) and Legendre polynomials up to a certain order (to allow "wiggles" locally to account for missing complexity in the nominal background model).
- The procedure is validated using an ensemble generated from the background-only fit model to the data.
- The search is currently blinded (hence the cut-off at +2 on the figures).

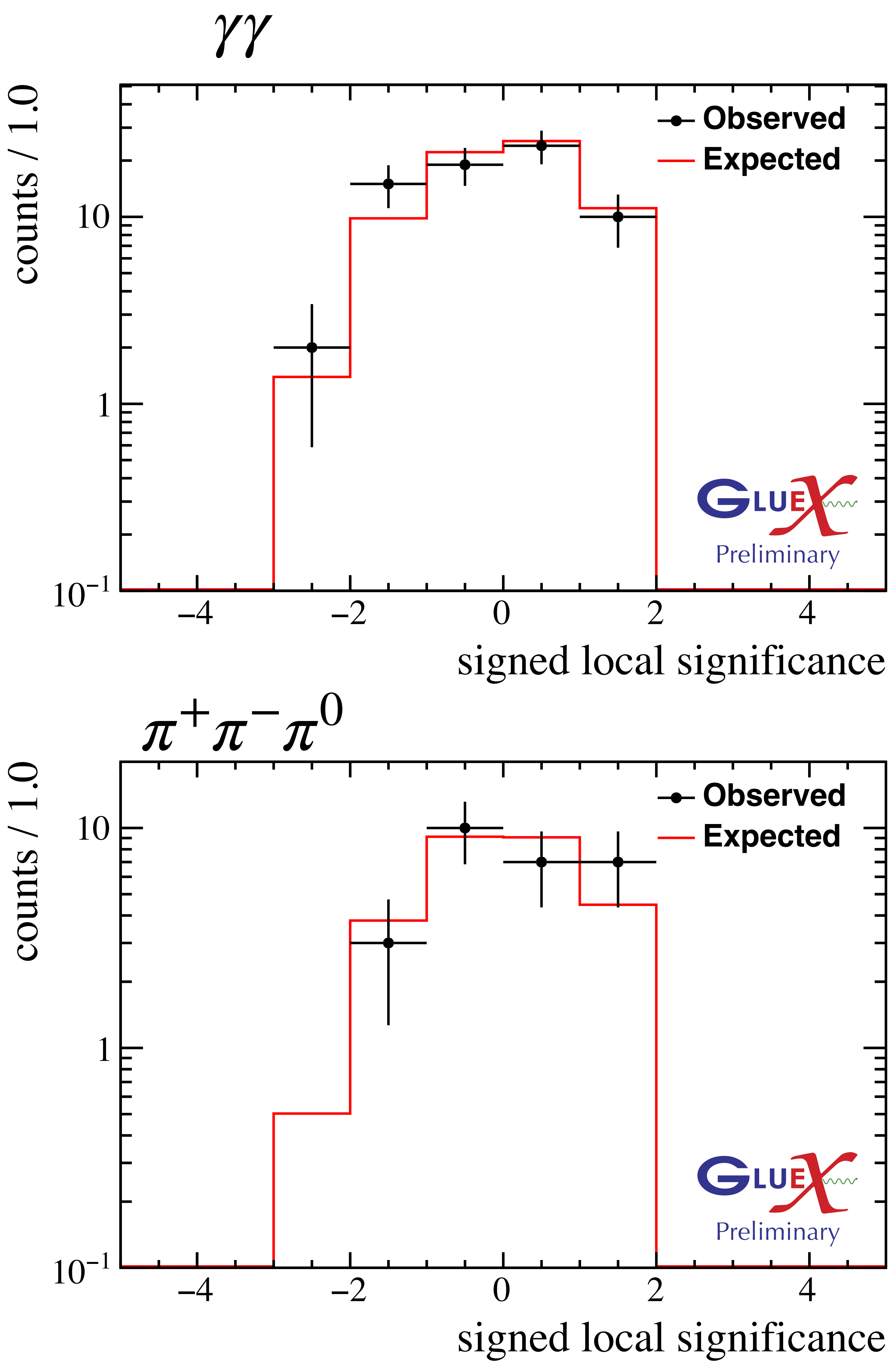

[5] M. Williams. JINST 12, P09034 (2017). arXiv: 1705.03578
[6] LHCb collaboration. PRL 120, 061801 (2018). arXiv: 1710.02867
[7] LHCb collaboration. PRL 124, 041801 (2020). arXiv: 1910.06926
[8] LHCb collaboration. JHEP 10 (2020)156. arXiv: 2007.03923
[9] C. Cesarotti, Y. Soreq, M. J. Strassler, J. Thaler, W. Xue. PRD 100, 015021 (2019). arXiv:1902.04222
[10] J. Landay, M. Mai, M. Döring, H. Haberzettl, K. Nakayama. PRD 99, 016001 (2019). arXiv:1810.00075